

## References

- <sup>1</sup>Marotta, E. E., and Fletcher, L. S., "Thermal Contact Conductance of Selected Polymeric Materials," *Journal of Thermophysics and Heat Transfer*, Vol. 10, No. 2, 1996, pp. 334–342.
- <sup>2</sup>Mikic, B. B., "Thermal Contact Conductance; Theoretical Considerations," *International Journal of Heat and Mass Transfer*, Vol. 17, 1974, pp. 205–214.
- <sup>3</sup>Cooper, M., Mikic, B. B., and Yovanovich, M. M., "Thermal Contact Conductance," *International Journal of Heat and Mass Transfer*, Vol. 12, 1969, pp. 279–300.
- <sup>4</sup>Parihar, S. K., and Wright, N. T., "Thermal Contact Resistance at Elastomer to Metal Interfaces," *International Communications in Heat and Mass Transfer*, Vol. 24, No. 8, 1997, pp. 1083–1092.
- <sup>5</sup>Makushkin, A. P., "Study of Stress-Strain of Polymer Layer During Spherical Indenter Penetration," *Trenie I Izmos*, Vol. 5, No. 5, 1984, pp. 823–832.
- <sup>6</sup>Greenwood, J. A., and Williamson, J. B. P., "Contact of Nominally Flat Surfaces," *Proceeding of the Royal Society of London, Series A: Mathematical and Physical Sciences*, Vol. A295, 1966, pp. 300–319.

# Impingement Heat Transfer Measurements Under an Array of Inclined Jets

Srinath Ekkad\*

Louisiana State University, Baton Rouge, Louisiana 70803  
and

Yizhe Huang† and Je-Chin Han‡

Texas A&M University, College Station, Texas 77843

## Introduction

JET impingement is a commonly used technique for heat transfer enhancement. Several applications such as heat treatment of metals, paper drying, electronic component cooling, and turbine component cooling have benefitted from the high heat transfer rate associated with jet impingement. Several geometrical and flow parameters are known to affect the heat transfer rate for jet impingement. Perry,<sup>1</sup> Chupp et al.,<sup>2</sup> Kercher and Tabakoff,<sup>3</sup> Flourschuetz et al.,<sup>4,5</sup> Behbahani and Goldstein,<sup>6</sup> and Downs and James<sup>7</sup> studied the effects of various parameters relating to jet impingement heat transfer. All of these studies had orthogonal jet impingement. They summarized the effects of geometry, temperature, interference and crossflow, turbulence levels, surface curvature, and nonuniformity of jet array on heat and mass transfer.

Goldstein and Franchett,<sup>8</sup> Steven and Webb,<sup>9</sup> and Ichimaya<sup>10</sup> studied the effects of inclined jet impingement and found that inclined jets produce less heat transfer enhancement than orthogonal jets. However, they did not investigate the effects of crossflow on inclined jet impingement. Huang et al.<sup>11</sup> studied the effect of crossflow direction on jet impingement heat transfer for orthogonal impinging jets. They reported the highest heat transfer coefficients for the jets where the crossflow exits in both directions. The present study investigates the same crossflow effects of Huang et al.<sup>11</sup> for inclined jet impingement.

The present study provides detailed surface heat transfer coefficient distributions for the target plate using a transient liquid crystal technique. This is the same methodology applied by the same group

of authors as in the studies by Huang et al.<sup>11</sup> and Ekkad et al.<sup>12</sup> In the present study, the effect of crossflow direction and jet inclination angle is presented for a single jet average Reynolds number of  $1.28 \times 10^4$ .

## Test Description and Apparatus

A detailed description of the test setup and instrumentation is provided by Huang et al.<sup>11</sup> The test section has been modified to accept jet impingement plates with inclined angled holes. There are 48 impingement holes of 0.635-cm diam arranged in an array of 12 columns and 4 rows. The jet-to-jet spacing  $S/d$  is four hole diameters. The jet plate to target plate spacing  $H/d$  (shortest distance between jet hole plate and target plate) is three hole diameters. The flow enters the pressure plenum through a narrow channel and exits through the impingement holes and impinges on the target surface. The flow exit (crossflow) direction can be altered by changing the discharge openings after impingement. Figure 1 shows the schemes of the impinging jets at  $\pm 45$  deg to the vertical on to the target plate. Cases 1–3 are for different crossflow directions for the +45-deg angled jets, and cases 4–6 are for different crossflow directions for the –45-deg angled jets. The axial location is measured from the inlet side of the pressure plenum before impingement. The plate length  $X$  is normalized with the hole diameter  $d$  from 0 to 48. The hole  $L/d$  ratio is 1.0 for the orthogonal jets and is 1.41 for the inclined jets. The hole length is not long enough to provide a fully developed and directed jet. However, the jet appears to be inclined sufficiently to provide different surface heat transfer results than for the orthogonal jets.

To avoid redundancy, details on the experimental technique and test procedure are not repeated. Huang et al.<sup>10</sup> and Ekkad et al.<sup>11</sup> describe the test section, experimental technique, and testing procedure in detail. A transient liquid crystal technique is used to obtain the two-dimensional surface heat transfer coefficient distributions. The test surface is coated with a thin layer of thermochromic liquid crystals. A heated flow is suddenly directed into the test section. The time of color change from colorless to green at every pixel location on the target surface is measured using the image processing system. The heat transfer coefficient at every location is calculated using the one-dimensional transient conduction equation and a semi-infinite solid assumption. The average experimental uncertainty in the heat transfer coefficient measurement is around  $\pm 6.4\%$  with a maximum of around  $\pm 10\%$  near edges.

## Results and Discussion

Figure 2 presents the detailed Nusselt number ( $Nu = hd/k_{air}$ ) distributions on the target plate for the six cases shown in Fig. 1 at a jet average Reynolds number ( $Re_j = \rho V_j d / \mu$ ) of  $1.28 \times 10^4$ . The results are presented from  $X/d = 3.5$  to 44.5. The total length to jet hole diameter ratio of the target plate is 48. The measurements are presented over the entire span of the test section,  $Y/d = 24$ . Figure 2a shows the detailed Nusselt number distributions for the

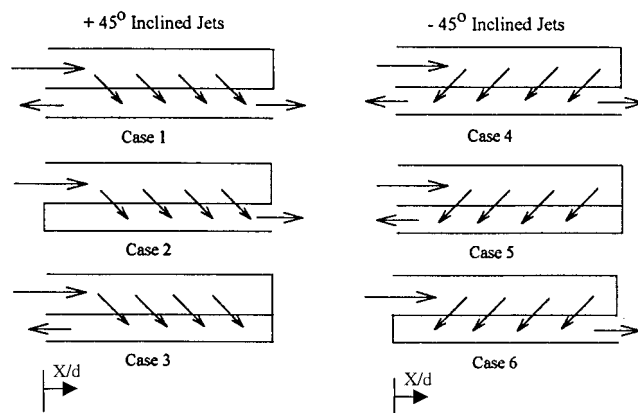


Fig. 1 Schematic of the inclined jet geometry and crossflow directions, cases 1–6.

Received 9 August 1999; revision received 19 November 1999; accepted for publication 24 November 1999. Copyright © 2000 by the American Institute of Aeronautics and Astronautics, Inc. All rights reserved.

\*Assistant Professor, Mechanical Engineering Department. Member AIAA.

†Research Assistant, Department of Mechanical Engineering; currently Project Engineer, Motorola, Inc., Austin, TX 78712.

‡Heat Transfer Research Institute Professor, Department of Mechanical Engineering. Associate Fellow AIAA.

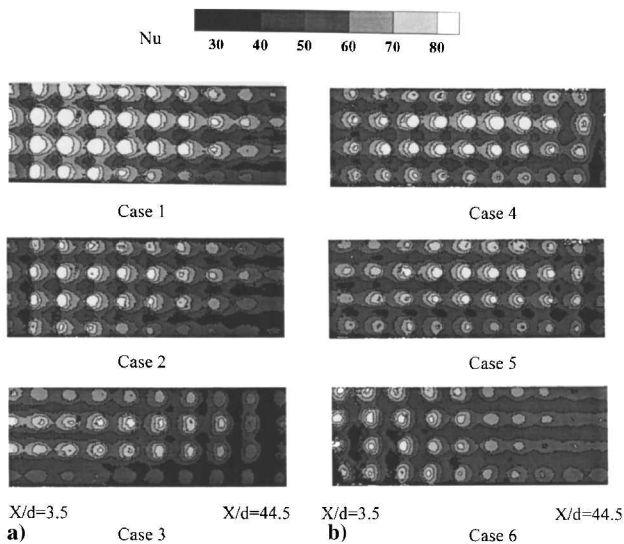
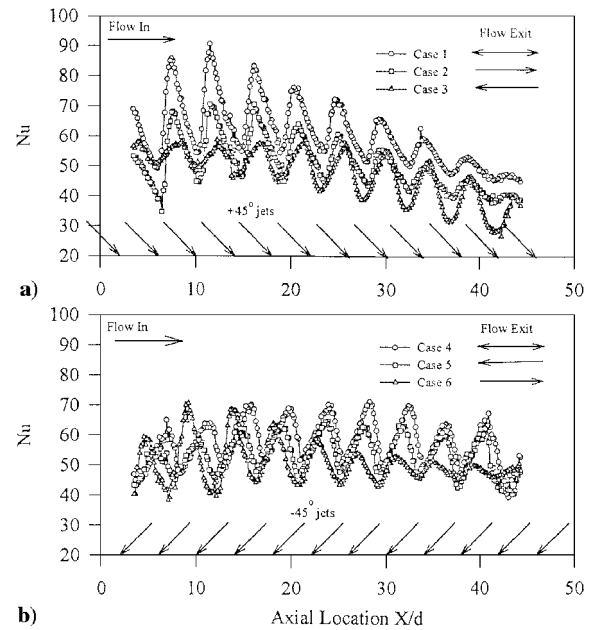


**Fig. 2 Detailed Nusselt number distributions for all cases shown in Fig. 1.**

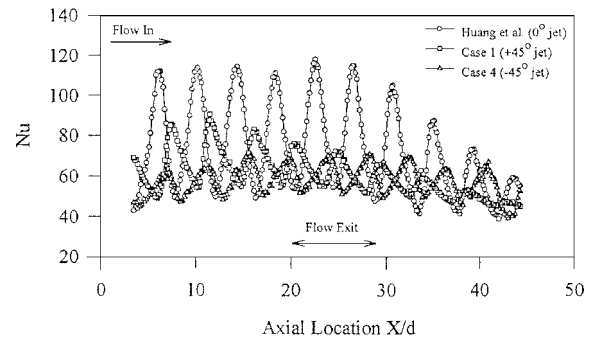
+45-deg impingement angle with different crossflow orientations. Case 1, where the flow exits in both directions after impingement, provides the highest Nusselt numbers for most of the test surface. This may be due to the minimum crossflow effects in the center of the channel because the flow exits in both directions. The crossflow originates around  $X/d = 21$  (Huang et al.<sup>11</sup>) for this case. The Nusselt numbers are highest around  $X/d \sim 8-30$ . Nusselt numbers decrease with increasing and decreasing  $X/d$  from around the middle of the channel as the crossflow effect increases and pushes the jets away from the surface. Both cases 2 and 3 provide lower Nusselt numbers compared to case 1. For cases 2 and 3, the crossflow develops from the closed end of the channel to the exit. If the angle of the jets is in the direction of the crossflow, as is for case 2, the decrease in Nusselt numbers is significant at large  $X/d$  locations. However for case 3, the heat transfer coefficient is also lower at larger  $X/d$ . This may be because most of the flow exits through the holes near the exit at small  $X/d$ , and that causes reduced impingement near the closed end. The crossflow and jet inclination angle are opposed to each other for case 3, causing higher heat transfer coefficients for the jets impinging near the exit end. Because of this, the impinging jets closer to the exit get swept away from the surface, and this caused reduced Nusselt numbers on the target surface. The jets appear to stretch and merge due to the combined effect of crossflow and inclination at the exit planes.

Figure 2b shows the detailed Nusselt number distributions for the -45-deg impingement angle with different crossflow orientations. As for the +45-deg impingement, Nusselt numbers are highest for case 4, where the flow exits in both directions. Cases 5 and 6 show distributions similar to those of cases 2 and 3 with only one side open for the flow exit after impingement. For case 5, the jet angle and crossflow directions are the same. This causes the Nusselt numbers to decrease toward the exit. For case 6, the jet angle and crossflow are in opposite directions. This causes significantly lower Nusselt numbers near the exit as the jets impinging into the crossflow are swept away from the surface.

Figure 3 presents the span-averaged Nusselt number distributions for all of the cases. Figure 3a shows the effect of crossflow exit direction for the jets inclined at  $\pm 45$  deg. The exit directions for each case are clearly indicated. Nusselt number distributions show periodic peaks where the jets impinge and periodic lows in the regions between the jets. As crossflow increases, the jets are swept away reducing impingement and, thus, reducing the differences between the peaks and the valleys. Case 1 shows the highest Nusselt numbers decreasing toward the large  $X/d$  side. Case 2 shows similar distributions with the crossflow exit toward the large  $X/d$  end. However, case 3 shows lower Nusselt numbers at large  $X/d$  even though the flow exits at  $X/d = 0$ . This may be due to flow deficit through the



**Fig. 3 Effect of crossflow direction on span-averaged Nusselt number distributions: a) +45-deg angle and b) -45-deg angle.**



**Fig. 4 Effect of jet angle on span-averaged Nusselt number distributions for crossflow exiting in both directions.**

impingement holes at large  $X/d$ . Huang et al.<sup>10</sup> explain this effect in detail.

Figure 3b shows the effect of crossflow exit direction for the jets inclined at -45 deg. The difference between cases 4 and 5 is smaller than that seen for cases 1 and 2. The jets are inclined against the main crossflow direction for case 4 causing reduced impingement in the middle of the channel compared to that for case 1. This impingement angle appears to provide uniform peak-to-valley Nusselt number distributions along the entire streamwise distance of the channel for both cases 4 and 5. For case 6, there is a low Nusselt number region at large  $X/d$  due to a flow deficit.

Figure 4 compares the angled impingement data from this paper with orthogonal jet impingement data from Huang et al.<sup>11</sup> for a crossflow orientation where the flow exits in both directions to determine the best of the three jet angle configurations. The orthogonal jet impingement clearly provides highest Nusselt numbers underneath the jets. The peak-to-valley differences are significant for orthogonal impingement. Case 1 for +45-deg impingement produces higher Nusselt number at smaller  $X/d$  region compared to case 4 for -45-deg impingement. At the large  $X/d$  region, where crossflow effects are significant, all three impingement angles produced similar Nusselt number levels. In accord with previous published studies on jet impingement,<sup>1-6</sup> jet plate to target plate distance significantly affects heat transfer augmentation. For inclined jets, the jet distance from the hole exit to target surface is longer than for orthogonal jets. Therefore, the inclined jets produce around ~12–20% lower test-plate-averaged (overall average) Nusselt numbers for jet distances about 41% longer than for orthogonal jets.

### Conclusions

The effects of impinging jet angle on target surface heat transfer distributions for an array of impinging jets are presented. The detailed distributions clearly indicate the jet angle and crossflow exit direction effects. The crossflow effects for orthogonal jets are discussed in detail by Huang et al.<sup>11</sup> The span-averaged Nusselt number distributions show periodic peak and valley distributions with decreasing values along the crossflow direction. Nusselt number distributions are significantly affected by the combination of jet exit angle and crossflow exit direction. More important, orthogonal jets provide higher Nusselt number underneath the impingement location compared to angled jets. Angled jets have ~40% longer impingement distances from the hole exit to the target plate and produce 12–20% lower overall-averaged Nusselt numbers. Although local differences in Nusselt numbers are significantly affected by jet inclination, the inclined jets produce more uniform Nusselt number distributions than the orthogonal jets, which may be considered a positive result for some practical applications.

### References

- <sup>1</sup>Perry, K. P., "Heat Transfer by Convection from a Hot Gas Jet to a Plane Surface," *Proceedings of the Institute of Mechanical Engineers*, Vol. 168, London, 1954, pp. 775–780.
- <sup>2</sup>Chupp, R. E., Helms, H. E., McFadden, P. W., and Brown, T. R., "Evaluation of Internal Heat Transfer Coefficients for Impingement Cooled Turbine Blades," *Journal of Aircraft*, Vol. 6, No. 1, 1969, pp. 203–208; also AIAA Paper 68-564, 1968.
- <sup>3</sup>Kercher, D. M., and Tabakoff, W., "Heat Transfer by a Square Array of Round Air Jets Impinging Perpendicular to a Flat Surface Including the Effect of Spent Air," *Journal of Engineering for Power*, Vol. 92, No. 1, 1970, pp. 73–82.
- <sup>4</sup>Florschuetz, L. W., Truman, C. R., and Metzger, D. E., "Streamwise Flow and Heat Transfer Distribution for Jet Array Impingement with Crossflow," *Journal of Heat Transfer*, Vol. 103, No. 2, 1981, pp. 337–342.
- <sup>5</sup>Florschuetz, L. W., Metzger, D. E., Su, C. C., Isoda, Y., and Tseng, H. H., "Heat Transfer Characteristics for Jet Array Impingement with Initial Crossflow," *Journal of Heat Transfer*, Vol. 106, No. 1, 1984, pp. 34–41.
- <sup>6</sup>Behbahani, A. I., and Goldstein, R. J., "Local Heat Transfer to Staggered Arrays of Impinging Circular Air Jets," *Journal of Engineering for Power*, Vol. 105, No. 3, 1983, pp. 354–360.
- <sup>7</sup>Downs, S. J., and James, E. H., "Jet Impingement Heat Transfer—A Literature Survey," American Society of Mechanical Engineers, Paper 87-HT-35, Nov. 1987.
- <sup>8</sup>Goldstein, R. J., and Franchett, M. E., "Heat Transfer from a Flat Surface to an Oblique Impinging Jet," *Journal of Heat Transfer*, Vol. 110, No. 1, 1988, pp. 84–90.
- <sup>9</sup>Steven, J., and Webb, B. W., "The Effect of Inclination on Local Heat Transfer Under an Axisymmetric Free Liquid Jet," *International Journal of Heat and Mass Transfer*, Vol. 34, No. 7, 1991, pp. 1227–1236.
- <sup>10</sup>Ichimaya, K., "Heat Transfer and Flow Characteristics of an Oblique Turbulent Impinging Jet Within Confined Walls," *Journal of Heat Transfer*, Vol. 117, No. 2, 1995, pp. 316–322.
- <sup>11</sup>Huang, Y., Ekkad, S. V., and Han, J. C., "Local Heat Transfer Coefficient Distribution Under an Array of Impinging Jets Using a Transient Liquid Crystal Technique," *Journal of Thermophysics and Heat Transfer*, Vol. 12, No. 1, 1998, pp. 73–79.
- <sup>12</sup>Ekkad, S. V., Huang, Y., and Han, J. C., "Impingement Heat Transfer on a Target Plate with Film Cooling Holes," *Journal of Thermophysics and Heat Transfer*, Vol. 13, No. 4, 1999, pp. 522–528.